


Article

A Constantly Updated Flood Hazard Assessment Tool Using Satellite-Based High-Resolution Land Cover Dataset Within Google Earth Engine

Alexandra Gemitzi ¹, Odysseas Kopsidas ¹, Foteini Stefani ², Aposotolos Polymeros ³ and Vasilis Bellos ^{1,*}

¹ Department of Environmental Engineering, Democritus University of Thrace, 67100 Xanthi, Greece; agkemitz@env.duth.gr (A.G.); odykopsi@yahoo.gr (O.K.)

² National School of Public Administration and Local Government, 17778 Athens, Greece; efistefani1@gmail.com

³ Ministry of Rural Development and Food, 10176 Athens, Greece; apolymeros@minagric.gr

* Correspondence: vbellos@env.duth.gr

Abstract: This work aims to develop a constantly updated flood hazard assessment tool that utilizes readily available datasets derived by remote sensing techniques. It is based on the recently released global land use/land cover (LULC) dataset Dynamic World, which is readily available, covering the period from 2015 until now, as an open data source within the Google Earth Engine (GEE) platform. The tool is updated constantly following the release rate of Sentinel-2 images, i.e., every 2 to 5 days depending on the location, and provides a near-real-time detection of flooded areas. Specifically, it identifies how many times each 10 m pixel is characterized as flooded for a selected time period. To investigate the fruitfulness of the proposed tool, we provide two different applications; the first one in the Thrace region, where the flood hazard map computed with the presented herein approach was compared against the flood hazard maps developed in the frames of the EU Directive 2007/60, and we found several inconsistencies between the two approaches. The second application focuses on the Thessaly region, aiming to assess the impacts of a specific, unprecedented storm event that affected the study area in September 2023. Moreover, a new economic metric is proposed, named maximum potential economic loss, to assess the socioeconomic implications of the flooding. The innovative character of the presented methodology consists of the use of remotely sensed-based datasets, becoming available at increasing rates, for developing an operational instrument that defines and updates the flood hazard zones in real-time as required.

Keywords: flood hazard; remote sensing; dynamic world; land cover; Google Earth Engine



Citation: Gemitzi, A.; Kopsidas, O.; Stefani, F.; Polymeros, A.; Bellos, V. A Constantly Updated Flood Hazard Assessment Tool Using Satellite-Based High-Resolution Land Cover Dataset Within Google Earth Engine. *Land* **2024**, *13*, 1929. <https://doi.org/10.3390/land13111929>

Academic Editor: Antonio Miguel Martínez-Graña

Received: 24 October 2024
Revised: 6 November 2024
Accepted: 11 November 2024
Published: 16 November 2024



Copyright: © 2024 by the authors. Licensee MDPI, Basel, Switzerland. This article is an open access article distributed under the terms and conditions of the Creative Commons Attribution (CC BY) license (<https://creativecommons.org/licenses/by/4.0/>).

1. Introduction

Floods are one of the natural disasters that pose a real threat to communities all over the world, especially in areas of low altitude with mild slopes and in coastal zones, impacting thus significantly human life. Floods may result in loss of human life, property damage, infrastructure damage, and subsequent economic losses [1–3]. Another serious flood implication is the displacement of people, which can be temporary or long-term, depending on the severity of the flood and the availability of resources to support those who have been displaced [4].

Flooding can also cause severe property damage, which lowers property values [5] but also can directly damage or obstruct the factors of production labor and physical capital [6]. They can harm all productive activities, such as farmland and crops, reducing agricultural output and raising food prices, manufacturing, and tourism. Especially in regions with historical or cultural significance, floods can harm or destroy significant landmarks and artifacts, causing a loss of cultural heritage and possibly having an adverse effect on tourism and the local economy [7].

It is rather difficult to define a generic metric for flood impact with global use. There are several attempts with pros and cons. The most generic metric is the number of flood events [8], but it has the disadvantages that it does not include the severity of the event, whereas it depends on the records of each country. The hard metric is the number of fatalities [9], which also raises questions since it does not count the excess mortality [10]. A widely common metric is the transformation of the flood impact into monetary units. According to the European Environmental Agency, flood impact can be estimated in several ways related to Euros, such as the total losses, losses per area, losses per capita, insured losses and ratio of the insured losses, to the total losses [11]. If we specialize the latter framework to the agricultural sector, we can define several indicators, such as the direct damage estimation, which includes the cost of damaged crops, livestock, and farmland infrastructure or the losses per hectare of cultivated land.

Thus, there is a need for proactive flood disaster risk management [2], for any flood type like flash floods, riverine floods, and flooding in urban areas, which can be greatly facilitated nowadays by remotely sensed information [12]. The Sendai framework for disaster risk reduction 2015–2030 sets three main goals related to the anticipation of flood impacts, focusing on the prevention of risk creation, reduction of existing risk, and strengthening of the economic, social, health, and environmental resilience [13].

According to the EU Directive 2007/60 [14], flood risk is a function of the probability of the flood event and the flood hazard, namely the flood extent, the water depths, and the flow velocities at the inundated area. Flood hazard mapping is the main approach to highlight areas with a specific probability of flood occurrence, where proactive measures should be targeted in order to protect existing infrastructure but also human and natural capital. This can be influenced by various factors such as topography, climate, and land use.

The EU Directive 2007/60 [14] requires EU member states to take a number of measures to reduce the negative impacts of floods on human health, the environment, and economic activities, including the identification of areas at risk of flooding, the development of flood risk maps and management plans, and the implementation of flood risk reduction measures. Member states must also cooperate with each other on cross-border flood risks and take into account the potential impacts of climate change on flood risks [15]. As climate change is expected to bring more frequent extreme precipitation events, floods are expected to pose a serious threat for human society and the environment, and within this context, flood hazard mapping is of major importance for urban and spatial planning and land use management [16–18].

Flood risk takes into account both the probability of flooding occurring and the potential consequences of flooding. This includes the potential damage to human health, the environment, cultural heritage, and economic activity associated with a flood event [14]. Flood risk assessments are used to identify areas that are at higher risk of flooding and to develop strategies for mitigating and managing the risks. Thus, flood risk is often estimated as the product of the probability of flooding multiplied by the value of infrastructure or assets present in the vulnerable sites.

The U.S. Federal Emergency Management Agency (<https://www.fema.gov/flood-maps>, accessed on 10 November 2024) highlights the usefulness of flood maps and indicates that any place with a 1% chance or higher chance of experiencing a flood each year is considered to have a high risk. Those areas have at least a one in four chance of flooding during a 30-year mortgage.

There are several methods to identify flood-prone areas, but the main tool is numerical modeling. The conventional way is to identify the catchment that runoff to the vulnerable area and implement a hydrological rainfall-runoff model that derives a flood hydrograph at the catchment outlet. Then, this hydrograph comprises the input for a physics-based hydrodynamic model (either in two or one dimension) with which the flood wave is propagated. The output of this hydraulic model is the final inundated area.

Except for the latter framework, there are several approaches, such as multi-criteria decision-making tools, statistical methods, and machine learning techniques [16–18], that

can be incorporated in the general methodology. Regarding the planning for response measures, cost-benefit analysis can significantly aid the decision-making process for flood risk reduction and mitigation. Decision makers can use it to weigh the expenses of various flood mitigation strategies against their possible upside in terms of lowering the risk of losses and damage [19].

Previous research has shown that climate change requires diversification of strategies to tackle flood impacts, coupling the probability and consequences, and emphasizing the coordination between spatial planners and water managers [20]. Specifically, the poor coordination across various government levels, policy areas, and communities of stakeholders was highlighted as a bottleneck in the policy response for successful flood adaptation. Other researchers [21] indicated the need to shift from a merely structural intervention approach for flood anticipation to strategies incorporating also non-structural interventions focusing on the importance of community members in the adoption and implementation of flood policies. It is also shown that such instruments diversify responsibilities to many stakeholders (and not only government) and thus require a high level of social acceptability for their effective implementation [22].

As previously mentioned, the EU Directive 2007/60 is the main tool for the European Union to define the strategy and to derive the policies for flood management. However, this framework has some drawbacks: (a) The inundated areas are produced using numerical modeling, which in general suffers from uncertainties. Moreover, the low quality or even the lack of historical data from flood events makes the calibration of the required parameters not feasible, and hence uncertainty is increased; (b) flood hazard maps are one snapshot in a specific time moment, and they cannot incorporate all the changes that affect the flooded area, such as the land use modifications, the urbanization, the construction of several manmade structures, the rainfall variability over time, etc.

Therefore, there is a gap between this static tool of EU flood hazard maps and the real world, which changes every day. During the last few years, remote sensing (RS) techniques have increasingly been used to identify the inundated areas after a flood event. For example, researchers used Sentinel-1 images in order to assess the performance of hydraulic modeling in a historical flood event [23]. Other researchers developed the FLOMPY toolbox to identify flooded areas in the past using Sentinel-1 images [24], and they used synthetic aperture radar approaches to support flood modeling [25]. There are also works using Sentinel-1 images within the Google Earth Engine (GEE) platform in which they identified the flood susceptibility of an area, namely which areas are more vulnerable to being flooded based on historical and topographic data [26] or they focused on the built-up area effect on flooding.

We have to admit that RS products and therefore Dynamic World (DW) [27] also suffer from uncertainties, and they cannot replace the in situ measurements. However, it is impossible to monitor floods on large scales since the majority of the catchments in real-world conditions are ungauged. Therefore, RS products combined with the capabilities of cloud computing provided in GEE constitute promising tools to derive a dataset for a plausible check of the model-derived flood hazard maps.

Recently, the EU Joint Research Center released a global gridded (1 km) dataset [28] on river flood hazards regarding flooding along the river network for seven different flood return periods (from 1-in-10-years to 1-in-500-years) based on the LISFLOOD model [29]. To the best of our knowledge, flood hazard mapping is based on hydrological modeling, while there is no approach that uses remote-sensed and constantly updated images of flood data that can be used to assess the output of the EU flood hazard maps. In this work, a methodology for the assessment of flood hazards and the associated socioeconomic implications is presented based on the land cover dataset DW produced by artificial intelligence (AI) [27], which is updated constantly following the revisit time of Sentinel 2, i.e., two to five days, and provides information on flooded areas at a 10 m spatial resolution. The assessment is built within the GEE platform and evaluates the flooding probability at the pixel level, computing the number of times each pixel is categorized as flooded in the

DW dataset for a given time period. Moreover, a new index for quantifying the economic impact of flooding is proposed, which is named maximum potential economic loss (MPEL). This metric has the potential for assisting policy makers to define new measures and strategies as far as flood management is concerned.

The methodology is applied in the river basin district (RBD) of Thrace in NE Greece, and it was compared against the latest flood hazard maps developed for the study area according to the requirements of the EU Directive 2007/60 [14]. Our work highlights the advantages of using near-real time updated information on floods, complementary to the EU flood hazard maps which are derived for a specific time moment. Its simplicity makes it an ideal instrument to overcome barriers encountered between scientific advances and policy adjustments since it is implemented within a simple GEE code, and hence it is also readily available for use in other areas around the world. Besides, this is the first time a constantly updated flood hazard assessment tool becomes available for use by every interested stakeholder.

Apart from that, we also applied the tool in the region of Thessaly, Greece, in order to identify the flood impact after the recent catastrophe due to Storm Daniel, which hit the Mediterranean basin in early September of 2023.

2. Materials and Methods

2.1. Description of the Study Areas

Two different applications associated with floods are incorporated in the present work in order to demonstrate the applicability and usefulness of the DW approach for flood hazard mapping. The first application is focused on Thrace RBD (Figure 1a) and aims to demonstrate how the flood risk management plans of the EU 2007/60 [14] can be improved combined with the presented herein approach. The second application focuses on Thessaly RBD in Central Greece (Figure 1b), and it aims to demonstrate the impact assessment of a single flooding event.

Thrace (Figure 1a) is located in the northeastern part of Greece with an area of approximately 11,250 km² and borders to the east with Turkey and to the north with Bulgaria. The annual precipitation from 2013 to 2018 is reported to range from 522 mm to 677 mm [30], while the mean monthly air temperature ranges from a lowest of 4 °C (January) to the highest of 25 °C (August) [31]. The climate is characterized as Mediterranean with hot and dry summer periods, whereas most precipitation takes place from October to May. There are two major transboundary river systems (Evros and Nestos), having their basins mainly within Bulgaria and Turkey, but they runoff to Greece (the Evros River is the border line between Greece and Turkey). Except for these two large rivers, there are several minor river systems across the RBD. The soil types prevailing in the study area range from sandy loams to clays [32–34], indicating a high potential for flooding, especially in the low-land areas occupied by fine grain soil types like clays. Land cover changes during the study period are reported in [35] and indicate a slight decrease of approximately 4.5% of cropland areas and a 12% decrease in shrubland areas and an increase of approximately 3.5% and 11.5% of trees and grassland areas, respectively.

Regarding the geomorphology of the RBD, the south part is mainly plain and covers about 50% of the area, while the rest is mountainous or semi-mountainous. Due to the fact that half of the area is characterized by mild slopes, there are a lot of historical flood events. During the period 1990–2010, around 200 events were recorded, of which 35 were significant according to the taxonomy of the *Special Secretariat of Water* [36]. The criteria for this categorization are the number of fatalities, the total amount of compensations, and the inundated area. The majority of the events are found in the Evros river; however, there are several events distributed in the rest of the river systems. The preliminary flood risk assessment defined that an area of approximately 2350 km² of the RBD (namely about 20% of the total area), as shown in Figure 1, is vulnerable to flooding.

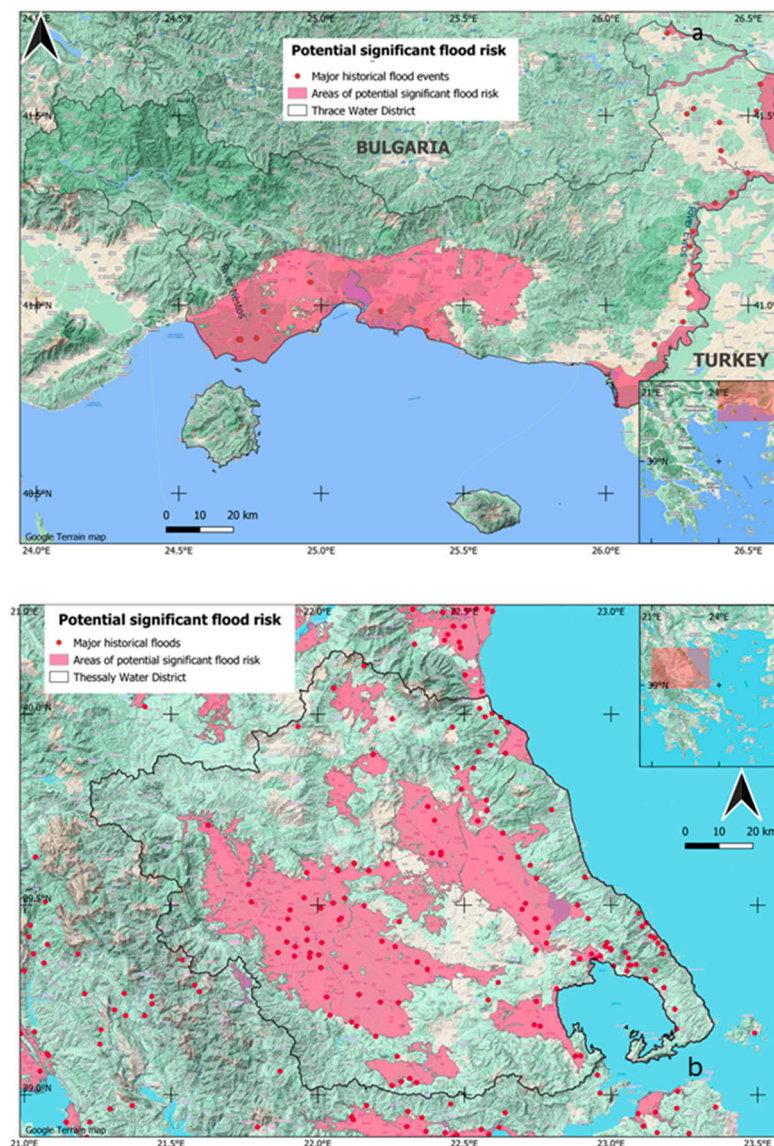


Figure 1. Location map of Thrace (a) and Thessaly (b) RBD and potential significant flood risk areas according to the EU Directive 2007/60 [10].

Thessaly RBD in Central Greece (Figure 1b) is generally a lowland area, while it is the main agricultural region of Greece. The area was affected by an unprecedented flood event that occurred in early September 2023 as a result of storm Daniel, which caused dramatic impacts mainly on the region of Thessaly in Central Greece. More than 750 mm of rainfall were recorded at the meteorological station of Zagora village near Mount Pelion, which approximates twice the annual rain of Athens [37]. During the flooding event, 729 km² were flooded.

The hydrographic network of Thessaly is mainly the Pineios River, which was the source of floods after the storm Daniel hit the area. The major impact from Pineios flooding was found in the western parts of Thessaly, which are characterized by very well-drained calcareous soils with coarse texture to moderately drained fine-textured soils [34].

2.2. Description of the Proposed Methodology for Flood Hazard Assessment

The flood hazard assessment approach presented herein builds on the DW global near-real-time land use/land cover product [27], which is the result of the joint effort of Google and the World Resources Institute. It is available through the GEE platform and can be viewed in the GEE public data catalog. The aim of this initiative was to release a global

LULC dataset, updated in near-real time, that could capture the dynamic nature of Earth's surface. A detailed description of the methodology and training material can be found on the DW web page [38]. DW is produced applying artificial intelligence (AI) principles using GEE and AI Platforms. It is based on the European Space Agency's Sentinel-2 Top of Atmosphere (TOA) images, which are classified into 9 land use/land cover classes using deep learning techniques. It has the spatial resolution of the original Sentinel-2 TOA product, i.e., 10 m, and it is updated globally every 2–5 days depending on the location, following the revisit time of Sentinel-2. The classification technique assigns per-pixel probabilities across nine land cover classes: water, trees, grass, crops, shrub and scrub, flooded vegetation, built-up area, barren ground, snow, and ice. The DW classification has been applied to all historic Sentinel-2 TOA images, i.e., from June 2015 and it is constantly updated as soon as new images become available.

Concerning the flood hazard assessment presented in this work, the class of flooded vegetation is of particular interest, as it describes vegetated conditions related to flooding. In the DW, each land cover class is represented by a different band. In this work, each pixel in every DW image of the study area, demonstrating the highest probability in the flooded vegetation class, is considered to be a flooded area, and it is assigned a value of 1, whereas in all other cases the pixel is assigned a zero value. Summing the values of each pixel across the whole time series, i.e., from June 2015 until today, corresponds to the number of times the specific pixel is viewed in flood conditions. As flooded areas are identified as those of any type of vegetated land cover other than water land cover, there is no need to filter for permanent water features as these are included exclusively in the water land cover class. All computations were performed within the GEE Platform with a Java Script code freely available using the link provided in the data availability section.

2.3. Comparison Against Conventional Flood Hazard Mapping

The main framework in order to derive strategic plans aiming to cope with floods is the European Union legislation and specifically the European Directive 2007/60 [14]. In this framework, the flood risk is assessed in three stages: (a) first, a preliminary flood risk assessment is performed on a coarse scale for every RBD in order to define which areas are more vulnerable to floods based on historical events, which in the case of Thrace and Thessaly RBDs are shown in Figure 1a and Figure 1b, respectively; (b) in the latter areas, flood hazard maps are derived for three different return periods, associated with high, medium, and low probability; (c) based on these maps, spatial flood risk is estimated incorporating hazards, exposure, and vulnerability.

The official flood hazard maps depict the flood-inundated area, and they are derived by synthetic storms produced for every return period using the alternate block method and the intensity–duration–frequency (IDF) curves of every RBD. For the transformation of these storms to flood hazard maps, hydrological modeling is coupled with hydrodynamic modeling. Specifically, the synthetic storms are transformed to runoff, using the well-known unit hydrograph theory coupled with the SCS method for the losses. Then, this runoff is the input for the hydrodynamic modeling which is based on either the 1D or 2D form of the shallow water equations, depending on the configuration of the case study. The output of these models is the flood hazard maps, namely the inundated area, for the return period of 50 (T50), 100 (T100), and 1000 (T1000) years of rainfall. It is noted that these maps were derived by different consortia of consultancies in each RBD, and hence with different approaches, software, etc.

2.4. Socioeconomic Implications

Flooding in the two examined RBDs can have indirect and direct expenses, including property damage and lost commercial activity [39]. These costs can include communication breakdowns and higher insurance rates. The daily activities of locals might be severely disrupted by flooding, including access to basic services, communication, and transportation, but also the environment is seriously impacted by destroying habitats, eroding land,

and contaminating streams. Many projects funded by the European Commission and the European Investment Bank focus on the protection of cities and mitigation of flood impacts in Greece and Bulgaria [40,41].

Regarding the Thrace RBD, the Evros River has caused many disastrous flood events in the recent past, notably during 2005, 2006, 2012, 2014, 2015, 2018 [42], and 2021 (<https://greekreporter.com/2021/02/01/firefighter-killed-as-floods-hit-greece-evros/>, accessed on 23 October 2024). It is worth noting that the 2006 floods in Evros River are presented in NASA's Earth Observatory (<https://earthobservatory.nasa.gov/images/6397/floods-along-the-evros-meric-river>), accessed on 23 October 2024). For Thessaly RBD, the presented herein application focuses on the impacts of a single devastating flood event, that of Storm Daniel (September 2023).

Within the present work, we computed the land cover types that were affected by flooding using the DW approach presented herein and compared it against the pan European-CORINE land cover dataset [43]. CORINE land cover offers a more detailed classification, i.e., 44 classes, compared to the 9 land cover classes of the DW. Thus, CORINE was the most suitable dataset to estimate economic losses. In the present work, the most recent CORINE land cover available was used, i.e., the 2018 dataset. In that way, the various sectors of the study area that were affected were determined, and the economic cost for the agricultural sector was evaluated based upon the standard output coefficients (abbreviated as SO), which are widely used by the European Commission and Member States. This is the average monetary value of the agricultural output at farm-gate price, in euros per hectare or per head of livestock [40]. Each coefficient is calculated for each product as an average value for a reference period of 5 years. The SO coefficients offer harmonization and comparability between member states for further impact assessment.

For the purposes of this paper, we propose the variable "Maximum Potential Economic Loss" (MPEL) as a measure of the maximum economic damage that can occur after a flood incident. The measure is straightforwardly linked with the risk-adverse nature of the farmers. Risk aversion is a relative concept and may vary according to the context and circumstances [44]. The methodology computes the annual costs of flooding at the pixel level and sums across all flooded pixels estimated costs, assuming flooded pixels are covered by water only once per year. Therefore, it does not account for multiple flooding events during a single year.

Specifically, MPEL of an agricultural product (crop or livestock) is the monetary value of the agricultural gross production at the farm-gate price. It is expressed as follows:

$$MPEL = S + V - DP \quad (1)$$

where S is the sales from farm use, farm consumption, and changes in stock; V is the value of the principle and any secondary products; DP is the direct payments (coupled, decoupled, and other payments), value added tax, and taxes on products.

Considering, however, that the methodology estimates the maximum potential economic loss, neglecting multiple floods in the same area balances the estimated costs, and we argue that this approach provides an average estimation of the economic loss caused by floods. It should be noted herein that the respective costs were not evaluated for the non-cultivated areas (forests or urban areas) since the majority of floods impacted agricultural land. However, a similar approach can be applied for any type of flooded area. The whole process is schematically depicted in Figure 2.

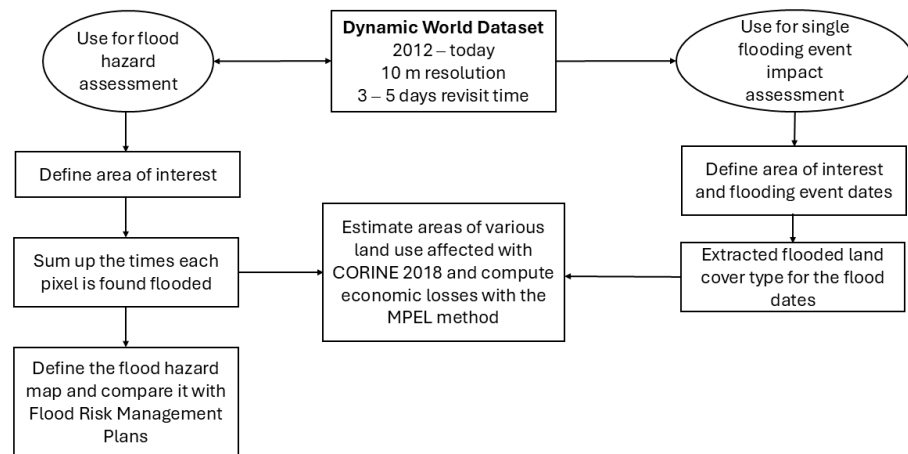


Figure 2. Flow chart of the flood hazard mapping approach.

3. Results

3.1. Comparison of DW with EU Flood Hazard Maps in Thrace RBD

Figure 3 shows the results obtained with the DW dataset in the Thrace RBD, whereas Figure 4 shows the frequency of flooding in various flooding areas. Figure 5 shows the 100-year return period flood areas, based on the flood hazard map of Thrace RBD [36]. Table 1 shows the various land cover areas affected at least once by flood events since 2015. Land cover types are provided according to the CORINE Label 2 nomenclature. It can be concluded thus that arable land comprises the vast majority of flooded areas, based on the analysis presented herein.

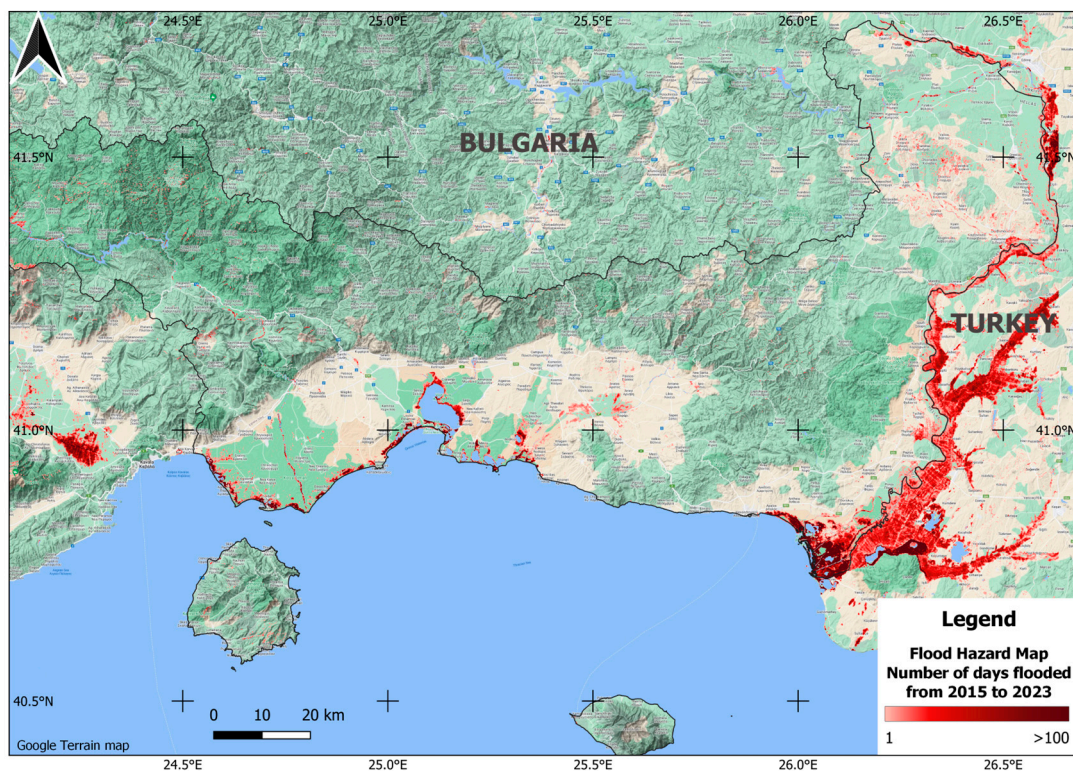


Figure 3. Flood Hazard Map of the broader Thrace RBD based on the methodology presented herein, covering the 2015–2023 period.

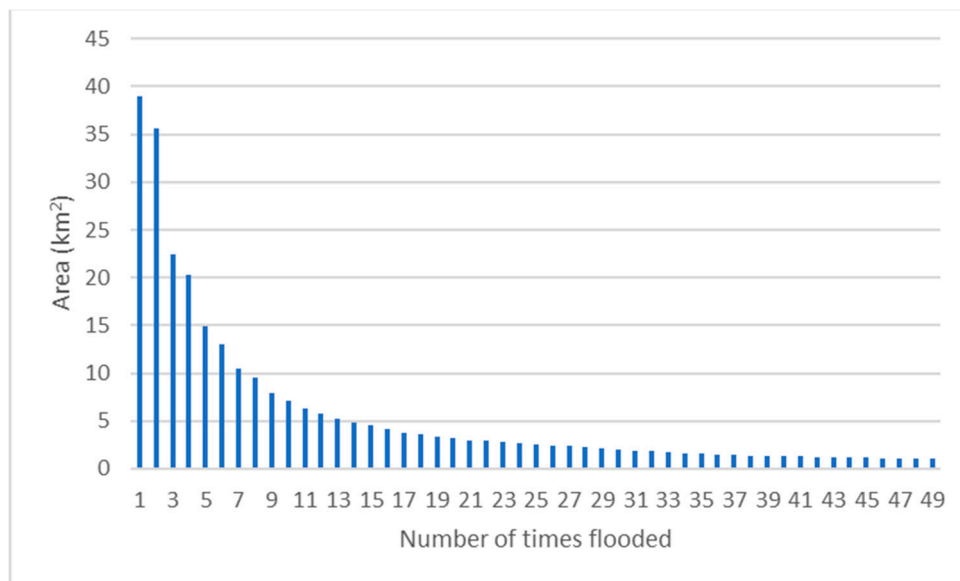


Figure 4. Flooded areas versus number of times flooded during 2015–2023 in Thrace RBD.

Table 1. CORINE land cover types of areas that flooded at least once since 2015 in Thrace RBD.

| Land Cover Type | Area (km ²) |
|---|-------------------------|
| Artificial, non-agricultural vegetated areas | 0.1 |
| Arable Land | 280.0 |
| Forests | 24.1 |
| Heterogeneous agricultural areas | 6.7 |
| Industrial, commercial and transport units | 0.6 |
| Mine, dump and construction sites | 0.1 |
| Pastures | 0.6 |
| Permanent Crops | 0.2 |
| Scrub and/or herbaceous vegetation associations | 8.4 |
| Urban fabric | 0.1 |

Comparison of the two independent datasets in Thrace RBD, which occupies an area of 11,250 km², revealed certain areas that correspond to 444.3 km² (Figure 6), where DW did not detect flood conditions, whereas the flood hazard map indicates them as inundated areas for the rainfall with a return period of 100 years. This is expected since the two datasets represent different things: (a) the first one is the inundated areas derived by model predictions using as an input the rainfall with a return period of 100 years; (b) the second one is the number of days in every 10 × 10 m pixel, which DW classified as flooded starting from June 2015. Given that, we cannot claim that DW underestimates or the flood hazard map overestimates flood hazard conditions. The areas that both datasets assign as flood cover 122.7 km². However, the most interesting outcome is that there is an area of 194.6 km², which has been observed as a flooded area at least once since 2015, in the DW approach only. This is a certain miss of the flood hazard map with a 100-year return period against reality. Taking into account that these maps are the main tool to define strategies and policies against floods, this discrepancy is of great importance. It is noted that those areas are observed along the eastern and northeastern areas of Thrace RBD, within the basin of River Evros.

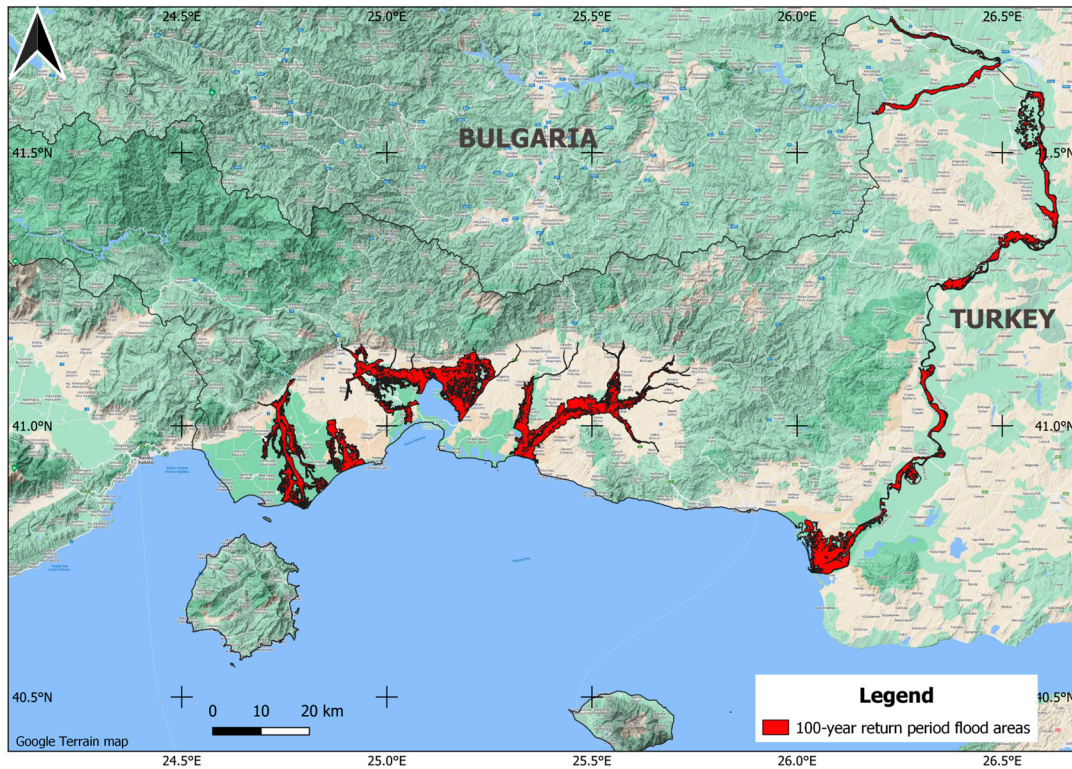


Figure 5. 100-year return period flood hazard map as defined in the flood management plan for Thrace RBD, Greece [28].

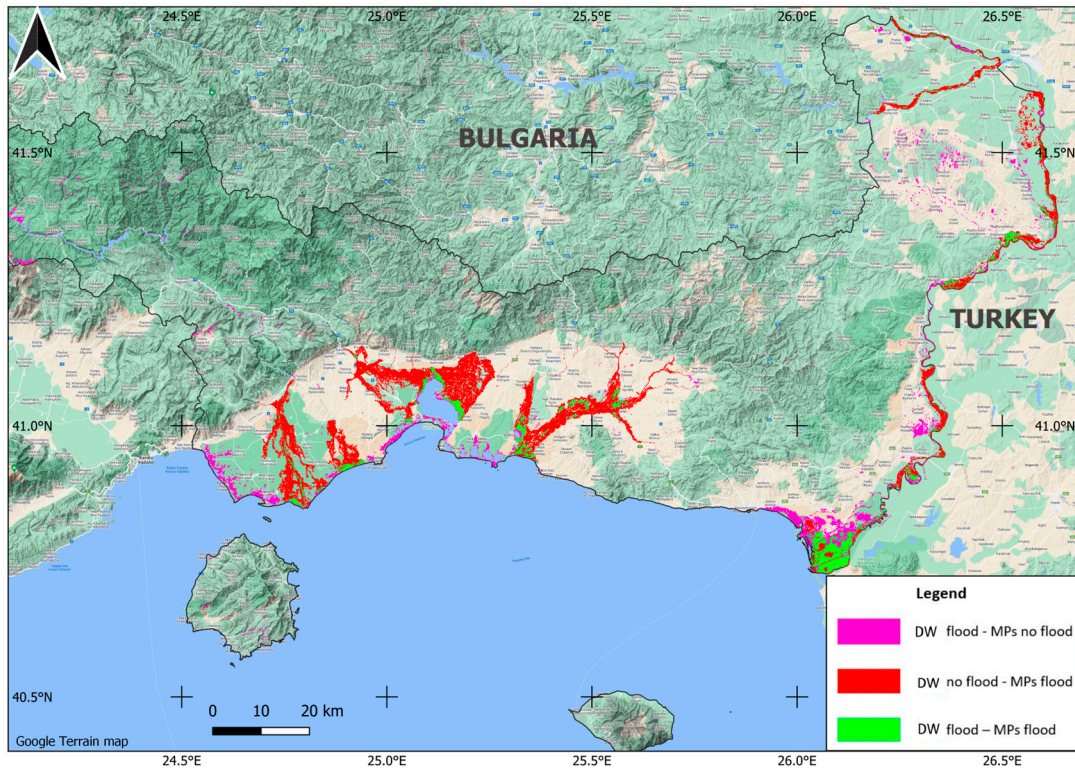


Figure 6. Comparison of the flood hazard map of the Thrace RBD based on the methodology presented herein against the 100-year flood hazard map based on the Flood Management Plan.

3.2. Seasonality of the Flooding in Thrace RBD

Apart from the spatial information which depicts the frequency with which flood occurs in an area, we also applied the DW tool for deriving the time series of the total flooded area in the region in order to investigate the seasonality of the phenomenon in the case study. Figure 7 depicts this information with a monthly step. Therein, one can see that March, followed by February, are the months with the highest flooded areas.

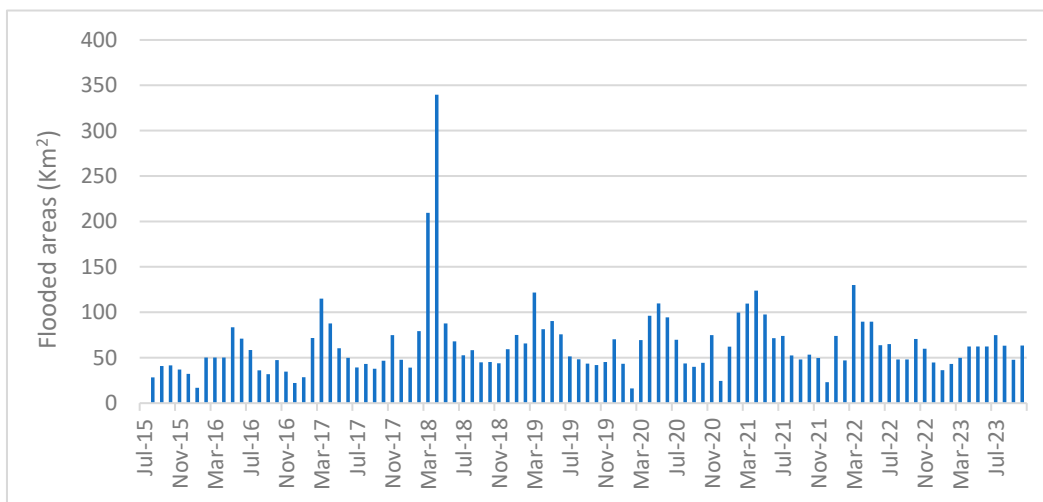


Figure 7. Time series of monthly flooded areas from 2015 to 2023 in Thrace RBD.

Next, we aggregated this information in an annual step. Figure 8 depicts the total annual flooded area. It can be seen that 2018 was the year that most flooding occurred, with over 300 km² flooded in the study area, while 2023 seems to be rather a dry year for the area.

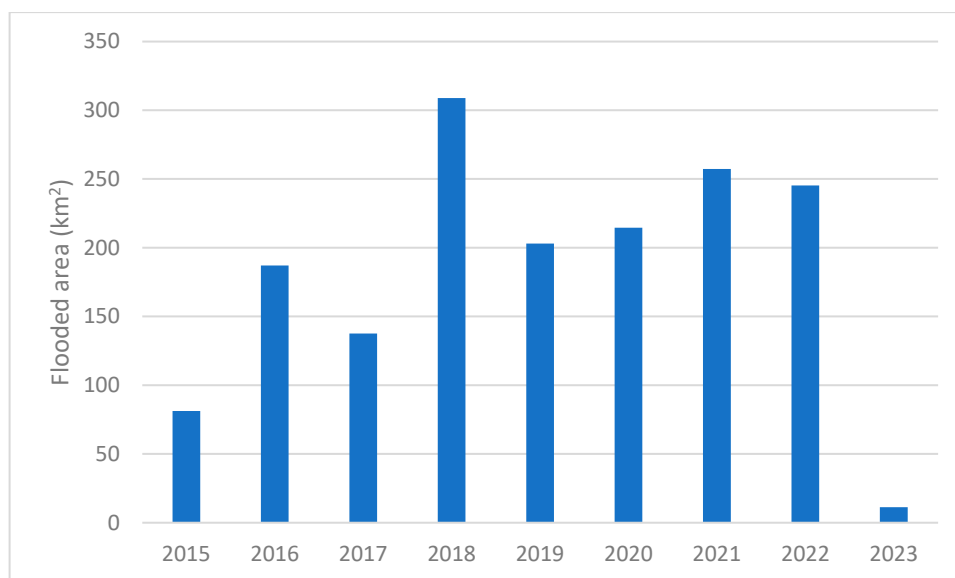


Figure 8. Annual flooded areas in Thrace RBD based on the DW approach.

3.3. Application of DW to the Recent Storm Daniel Flood in Region of Thessaly RBD

Except for the application of DW in Thrace, we defined the flooding area prior to and after the recent Storm Daniel [37,45] in Thessaly RBD. Specifically, Figure 9 depicts the results of the DW, while in Figure 10 the flooded area is plotted against how many times it is flooded, demonstrating that the flood impact of Daniel changed dramatically the

distribution of flooded areas, with more than 50 km² observed as flooded for the first time. Table 2 reports the various land cover types affected by the storm Daniel flooding event.

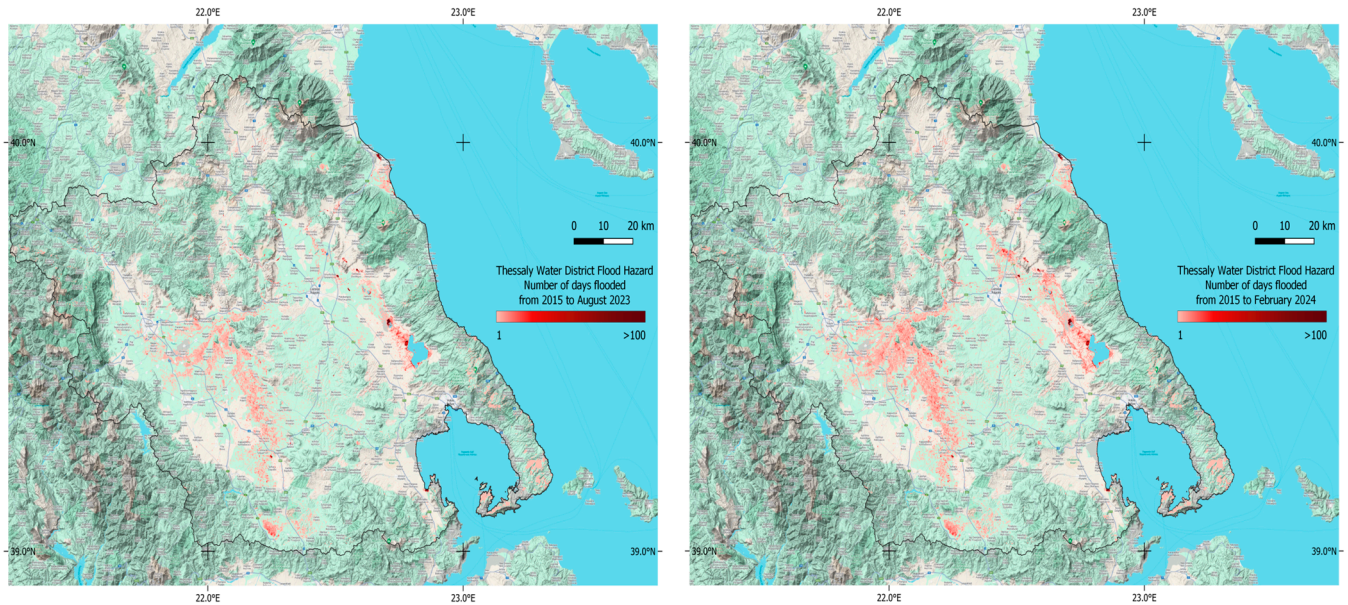


Figure 9. Flooded area prior to storm Daniel (left) and after storm Daniel (right).

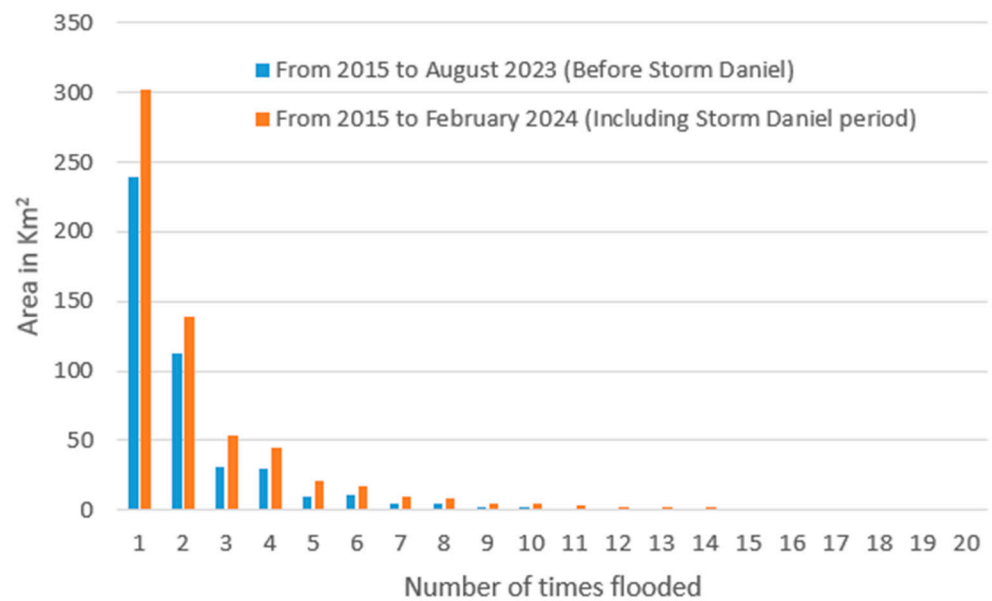


Figure 10. Flooded area against how many times is flooded before and after storm Daniel.

Table 2. CORINE land cover types of areas that flooded at least once since 2015 in Thessaly RBD.

| Land Cover Type | Area (km ²) |
|--|-------------------------|
| Artificial, non-agricultural vegetated areas | 2.5 |
| Arable Land | 321.0 |
| Pastures | 358 |
| Permanent Crops (vineyards, olive groves, fruit trees) | 50 |
| Urban fabric | 7.1 |

3.4. Implementation of the Proposed MPEL Index

Regarding the economic cost from flooding, the SO coefficients estimated as average values for the categories of cultivated land provided in Tables 1 and 2 are shown in Table 3. The data used to calculate MPEL cover a twelve-month production period. Consequently, longer impacts, e.g., those from the degradation of soil or loss of infrastructure, are not included in the MPEL computations. The sources of the data are the national farm structure survey (FSS) and the farm accountancy data network (FADN) of Greece provided by the Hellenic Organization of Agricultural Compensations [36].

Table 3. Economic cost of floods in cultivated lands estimated by SO coefficients.

| Cultivation Type | Cost MPEL Avg (€/hectare) |
|--|---------------------------|
| Arable Land and Heterogeneous agricultural areas | 3115.0 |
| Permanent crops | 5405.0 |
| Pastures and Scrub and/or herbaceous vegetation associations | 106.0 |

The computation of economic loss for Thrace RBD presented in Figure 11 provides an easily applicable relationship of flood cost according to the flooded area, which seems to be linear. Such relationships can be developed and applied in other RBD, providing readily available tools for flood-induced economic inference.

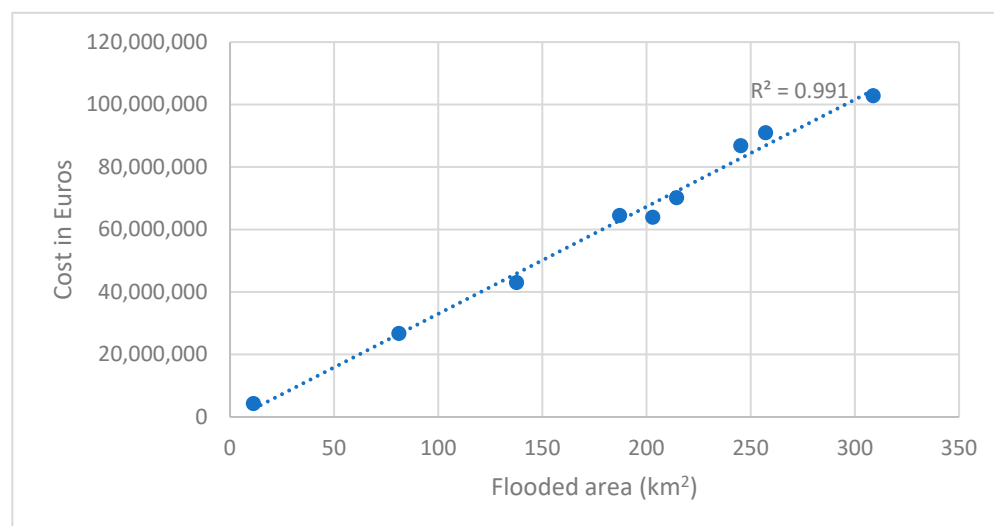


Figure 11. Total annual economic loss from flooding of cultivated land in Thrace RBD based on the extent of flooding areas according to the SO coefficients.

The seasonality of economic losses due to flooding is also investigated. Since we have derived the monthly time series of the flooded area in the Thrace RBD, we estimated for each month the total economic losses using the proposed MPEL index (Figure 12). The time period used for this analysis is from 2015 until 2023. As was expected from Figure 7, March, followed by February, are the months with the highest flood damage costs, since they are the months with the highest flooded area. It should be noted that not all crop types are impacted by winter floods in the area, and the MPEL computations could be improved by focusing on specific crops' damage costs for each season. This, however, requires updated data of registered farms for each season, which is not always available.

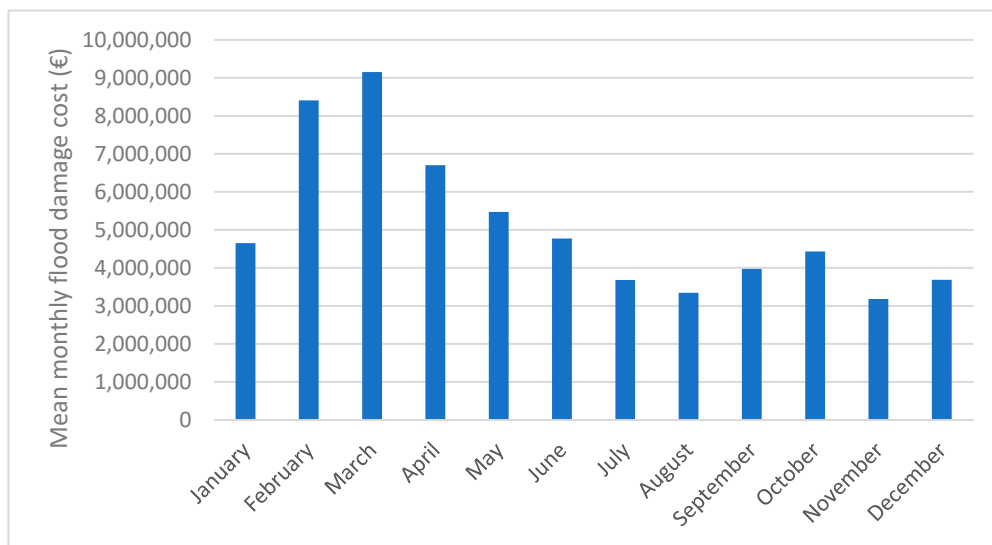


Figure 12. Mean monthly flood damage costs estimated in Thrace RBD with the MPEL method.

To check the potential of validating the MPEL methodology for flood damage cost estimation and to compare it with typical similar indices, we used the historical data of farm damage compensation (FDC) retrieved from the Hellenic Organization of Agricultural Compensations [46]. This comparison for 2015–2023 is depicted in Figure 13.

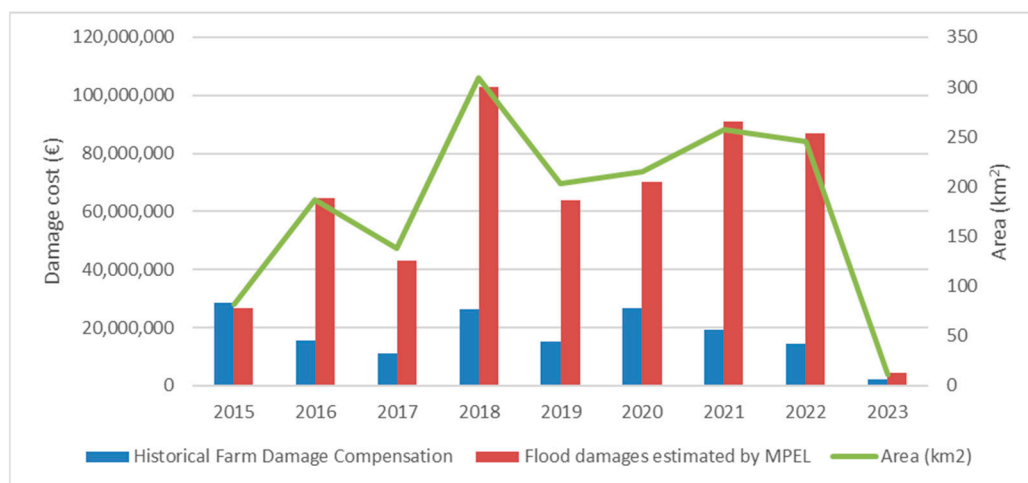


Figure 13. Comparison of historical farm damage compensations with flood damage costs by MPEL and associated flooded crop areas in Thrace RBD.

Although there is a clear correlation between historical farm damage compensations and those of the MPEL approach, the FDC is considerably lower. The only exception is the year 2015, but this specific year compensation might correspond to other types of damage and not only flood, since the term damage compensation in FDC refers to several types of damages, such as droughts, floods, extreme cold or hot conditions, pathogens, etc.

The reason for this discrepancy is that compensations are only provided to registered farms, and it amounts to 80% of the estimated actual damage. In the MPEL estimates, the CORINE 2018 land cover dataset was used for a coarse estimate of the maximum potential loss. In fact, MPEL is the monetary value of the agricultural gross production at the farm-gate price that expresses the real damage when the actual flood damage compensation is not available. In almost all years examined, the MPEL costs were considerably higher than the actual compensations granted.

Based on the associated computations for Thessaly RDB, using data reported in Tables 2 and 3, the flood damage to the agricultural sector is estimated, with the MPEL, to 130,811,300 €. Although the compensation computation process is still ongoing, according to estimates from the Ministry of Agricultural Development and Food Production, the total damage from Storm Daniel amounts to 300,000,000 EUR, comprising also the damages from livestock, decontamination works of the flooded areas, long-term loss of cropland areas, as well as compensations for loss of property [47]. Those specific damage costs are not included in the MPEL computations, which estimate only agricultural production damage costs. It is worth noting that according to many sources of information, the estimated cost of storm Daniel amounts to 4.5 billion EUR, with the majority of the amount estimated for flood protection works and restoration of damaged infrastructure [48].

All the above render FDC is a rather vague parameter, and it is based on the costs covered (e.g., agricultural, infrastructure, soil rehabilitation costs, etc.), duration of coverage (short-term losses or long-term rehabilitation works), and the estimation institute (e.g., Ministry of Agriculture, Regional Authorities, Municipalities, etc.), and sometimes those discrepancies minimize its usefulness for agricultural management, which is vulnerable from several natural disasters. On the other hand, the MPEL approach is a useful metric for quantifying the loss and developing new policies and strategies regarding flood risk mitigation. The versatility of the proposed index is also useful since it can be implemented either using the detailed information from the register of agricultural crops (which is not always available) or just with the land use maps and without other information.

4. Discussion

In this work, we developed an open tool based on remote sensed images obtained by the DW dataset, based on the classification of Sentinel 2 images, for identifying the time series of flooded areas with a continuous update. Our approach defines the number of times in a specified time period that each 10-m pixel in the area of interest is found flooded. In other words, it could be said that our approach defines the frequency of flooding, contributing thus to the flood hazard mapping using remotely sensed information. Traditionally, flood hazard maps are constructed using hydrological modeling forced by specified return period rainfall events, and we proved that the integration of the presented herein approach can improve the flood hazard mapping.

The presented approach is implemented in two RBDs in Greece, the Thrace RBD, where the result of the developed herein approach is compared with the corresponding flood hazard maps of the EU Directive 2007/60. It is found that there are discrepancies between the model product (i.e., the flood hazard maps) and the real-world picture, indicating that the conventional approach of flood hazard mapping could be substantially improved by integrating the results of the presented herein approach in the computations of flood hazard assessment. The second application is focused on Thessaly RBD, where storm Daniel caused an unprecedented flooding of approximately 730 km² during September 2023. The application in Thessaly highlighted the usefulness of the proposed approach in order to assess the impacts of specific flood events. Moreover, we introduced a new metric for quantifying the flood impact, namely the MPEL, and we implemented it in the same areas. Then, we compared this index with historical farm damage compensations, and we found that even though there is a clear correlation between these two indices, MPEL indicates that the economic loss was much higher than the historical data, which is expected since the paid compensations usually cover only a part of the actual losses. Our major findings are presented in the following paragraphs.

First, we shall keep in mind that the conventional flood hazard maps within the flood management plans are created on a probability basis using modeling tools and should be regarded as future potential flooding areas. In addition, these maps are derived assuming that there are no changes in the configuration of the vulnerable area. Our results indicated that there is space for improvement in those flood hazard maps combining information from satellite-based observations. The DW dataset approach, presented in this work, offers

a means of verification of the modeling results, especially by enhancing them in flooded areas that are not depicted in the flood hazard maps. Regarding the reliability of this dataset, it should be noted that it has been rigorously examined and tested with a large expert consensus dataset, and the results indicated top qualitative performance in each comparison category among the examined land cover datasets. Hence, the presented methodology, taking advantage of emerging techniques and datasets, helps policy makers acquire better and more timely information on flood hazard so as to improve the planning of protective measures.

Second, the Sentinel 2 mission has global coverage and covers all of Earth's continents and large islands, along with inland and coastal water bodies, with a revisit frequency of 5 days. However, cloud cover may restrict the acquisition of useful images, resulting in lower data availability in flooded areas with increased cloud cover, and therefore the results obtained with the DW dataset should be regarded as the minimum number of days the specific area is observed as flooded. It is very likely that some flood events are not detected by satellite observations due to cloud cover and are not included in the DW dataset. As the methodology is based on AI classification, there is always a slight possibility of misclassification, i.e., a dry pixel may appear falsely flooded and vice versa. Nevertheless, DW is an extensively evaluated dataset of high accuracy. Since it is a constantly updated dataset, its quality is expected to improve in the future versions. The probability for a specific area to have no RS history data is very low, and thus the methodology works at the global scale. Moreover, since the Sentinel 2 mission operates since 2015, the data history covers a relatively short time period, which however can be extended back to the early 1980s combining data from Landsat missions. This can be a very challenging future extension of the present work. Future research efforts should also focus on the combination with information from synthetic aperture radar imaging from Sentinel 1. Such an integration will enhance our flood hazard approach in terms of flood depth and improve its usefulness for impact assessment of specific flood events.

Finally, the growing production of freely available datasets related to environmental monitoring based on RS and AI technologies can be used to tackle the tremendous impacts on natural and human ecosystems due to flooding. The innovation of our approach consists of:

1. The development of an algorithm using the DW dataset within the GEE platform in order to utilize the high spatial resolution of the DW data.
2. The deployment of a user-friendly tool that can be used for the effective communication of scientific findings to government and policy makers but also to all community actors and will encourage social acceptability of improved flood anticipation policies.
3. The evidence of the usefulness of the tool, demonstrating the inadequacy of the river flood management plans against the outcome of the tool in the Thrace RBD.
4. The evidence of the usefulness of the DW approach for single flood events is demonstrated in the Thessaly RBD.
5. The new variable that is introduced, namely the maximum potential economic loss, can assist in quantifying the flood impact and, besides, has the potential to be an additional metric for developing flood protection scenarios by the several policy makers.

Author Contributions: Conceptualization, A.G. and V.B.; methodology, A.G., O.K., F.S., A.P. and V.B.; software, A.G. and A.P.; validation, A.G. and A.P.; formal analysis, A.G., O.K., F.S., A.P. and V.B.; investigation, A.G., O.K., F.S., A.P. and V.B.; resources, A.G., O.K., F.S., A.P. and V.B.; data curation, A.P. and V.B.; writing—original draft preparation, A.G., O.K., F.S., A.P. and V.B.; writing—review and editing, A.G. and V.B.; visualization, A.G., O.K., F.S., A.P. and V.B.; supervision, A.G. and V.B.; project administration, A.G. and V.B. All authors have read and agreed to the published version of the manuscript.

Funding: This research received no external funding.

Data Availability Statement: The Dynamic World dataset is produced for the Dynamic World Project by Google in partnership with National Geographic Society and the World Resources Institute. It is

available under a Creative Commons BY-4.0 license. The SO data set was provided by the Ministry of Rural Development and Food. Finally, the Google Earth Engine Java Script code is available at the following link: <https://code.earthengine.google.com/0840284cd1e3a07a09644fa5bf2e5f5f>, accessed on 23 October 2024.

Conflicts of Interest: The authors declare no conflicts of interest.

References

- Guha-Sapir, D.; Hoyois, P.; Below, R. Annual Disaster Statistical Review 2014 The Numbers and Trends Centre for Research on the Epidemiology of Disasters (CRED). 2014. Available online: https://www.cred.be/sites/default/files/ADSR_2014.pdf (accessed on 23 October 2024).
- Pabi, O.; Egyir, S.; Attua, E.M. Flood Hazard Response to Scenarios of Rainfall Dynamics and Land Use and Land Cover Change in an Urbanized River Basin in Accra, Ghana. *City Environ. Interact.* **2021**, *12*, 100075. [[CrossRef](#)]
- Venkataramanan, V.; Packman, A.I.; Peters, D.R.; Lopez, D.; McCuskey, D.J.; McDonald, R.I.; Miller, W.M.; Young, S.L. A Systematic Review of the Human Health and Social Well-Being Outcomes of Green Infrastructure for Stormwater and Flood Management. *J. Environ. Manag.* **2019**, *246*, 868–880. [[CrossRef](#)] [[PubMed](#)]
- International Federation of Red Cross and Red Crescent Societies. *Displacement in a Changing Climate Localized Humanitarian Action at the Forefront of the Climate Crisis*; International Federation of Red Cross and Red Crescent Societies: Geneva, Switzerland, 2021.
- Ismail, N.H.; Abd. Karim, M.Z.; Hasan Basri, B. A Hedonic Modelling of Land Property Value Based on the Effect of Flooding: A Case for Peninsular Malaysia. In *Proceedings of the Second International Conference on the Future of ASEAN (ICoFA) 2017*; Springer: Singapore; Volume 1, 2019; pp. 167–179.
- Sun, Q.; Mann, J.; Skidmore, M. The Impacts of Flooding and Business Activity and Employment: A Spatial Perspective on Small Business. *Water Econ. Policy* **2022**, *8*, 21400038. [[CrossRef](#)]
- Stefanidis, S.; Alexandridis, V.; Theodoridou, T. Flood Exposure of Residential Areas and Infrastructure in Greece. *Hydrology* **2022**, *9*, 145. [[CrossRef](#)]
- Gaume, E.; Bain, V.; Bernardara, P.; Newinger, O.; Barbuc, M.; Bateman, A.; Blaškovičová, L.; Blöschl, G.; Borga, M.; Dumitrescu, A.; et al. A Compilation of Data on European Flash Floods. *J. Hydrol.* **2009**, *367*, 70–78. [[CrossRef](#)]
- Kundzewicz, Z.W.; Kundzewicz, W.J. Mortality in Flood Disasters. In *Extreme Weather Events and Public Health Responses*; Springer: Berlin/Heidelberg, Germany, 2005; pp. 197–206.
- Hammer, C.C. Understanding Excess Mortality from Not-so-Natural Disasters. *Lancet Planet Health* **2018**, *2*, e471–e472. [[CrossRef](#)]
- European Environment Agency. *Economic Losses from Weather- and Climate-Related Extremes in Europe*; European Environment Agency: Copenhagen, Denmark, 2024.
- Ajmar, A.; Boccardo, P.; Broglia, M.; Kucera, J.; Giulio-Tonolo, F.; Wania, A. Response to Flood Events. In *Flood Damage Survey and Assessment*; Geophysical Monograph Series; American Geophysical Union: Washington, DC, USA, 2017; pp. 211–228. ISBN 9781119217930.
- United Nations Office for Disaster Risk Reduction. *Sendai Framework for Disaster Risk Reduction 2015–2030*; United Nations Office for Disaster Risk Reduction: Geneva, Switzerland, 2015.
- Directive 2007/60/EC*; EU Parliament Floods Directive. 2007.
- Omer, A.; Yuan, X.; Gemtzi, A. Transboundary Nile Basin Dynamics: Land Use Change, Drivers, and Hydrological Impacts under Socioeconomic Pathways. *Ecol. Indic.* **2023**, *153*, 110414. [[CrossRef](#)]
- Hosseini, F.S.; Choubin, B.; Mosavi, A.; Nabipour, N.; Shamshirband, S.; Darabi, H.; Haghghi, A.T. Flash-Flood Hazard Assessment Using Ensembles and Bayesian-Based Machine Learning Models: Application of the Simulated Annealing Feature Selection Method. *Sci. Total Environ.* **2020**, *711*, 135161. [[CrossRef](#)]
- Ran, J.; Nedovic-Budic, Z. Designing an Information Infrastructure for Policy Integration of Spatial Planning and Flood Risk Management. In *Environmental Information Systems*; IGI Global: Hershey, PA, USA, 2019; pp. 520–554.
- Rafiei-Sardooi, E.; Azareh, A.; Choubin, B.; Mosavi, A.H.; Clague, J.J. Evaluating Urban Flood Risk Using Hybrid Method of TOPSIS and Machine Learning. *Int. J. Disaster Risk Reduct.* **2021**, *66*, 102614. [[CrossRef](#)]
- Hudson, P.; Wouter Botzen, W.J. Cost–Benefit Analysis of Flood-Zoning Policies: A Review of Current Practice. *Wiley Interdiscip. Rev. Water* **2019**, *6*, e1387. [[CrossRef](#)]
- Vitale, C. Understanding the Shift toward a Risk-Based Approach in Flood Risk Management, a Comparative Case Study of Three Italian Rivers. *Environ. Sci. Policy* **2023**, *146*, 13–23. [[CrossRef](#)]
- Haque, C.E.; Azad, M.A.K.; Choudhury, M.U.I. Discourse of Flood Management Approaches and Policies in Bangladesh: Mapping the Changes, Drivers, and Actors. *Water* **2019**, *11*, 2654. [[CrossRef](#)]
- Raikes, J.; Henstra, D.; Thistlethwaite, J. Public Attitudes Toward Policy Instruments for Flood Risk Management. *Environ. Manag.* **2023**, *72*, 1050–1060. [[CrossRef](#)] [[PubMed](#)]
- Zotou, I.; Bellos, V.; Gkouma, A.; Karathanassi, V.; Tsihrintzis, V.A. Using Sentinel-1 Imagery to Assess Predictive Performance of a Hydraulic Model. *Water Resour. Manag.* **2020**, *34*, 4415–4430. [[CrossRef](#)]
- Karamvasis, K.; Karathanassi, V. FLOMPY: An Open-Source Toolbox for Floodwater Mapping Using Sentinel-1 Intensity Time Series. *Water* **2021**, *13*, 2943. [[CrossRef](#)]

25. Zotou, I.; Karamvavis, K.; Karathanassi, V.; Tsihrintzis, V.A. Potential of Two SAR-Based Flood Mapping Approaches in Supporting an Integrated 1D/2D HEC-RAS Model. *Water* **2022**, *14*, 4020. [CrossRef]
26. Mehravar, S.; Razavi-Termeh, S.V.; Moghimi, A.; Ranjgar, B.; Foroughnia, F.; Amani, M. Flood Susceptibility Mapping Using Multi-Temporal SAR Imagery and Novel Integration of Nature-Inspired Algorithms into Support Vector Regression. *J. Hydrol.* **2023**, *617*, 129100. [CrossRef]
27. Brown, C.F.; Brumby, S.P.; Guzder-Williams, B.; Birch, T.; Hyde, S.B.; Mazzariello, J.; Czerwinski, W.; Pasquarella, V.J.; Haertel, R.; Ilyushchenko, S.; et al. Dynamic World, Near Real-Time Global 10 m Land Use Land Cover Mapping. *Sci. Data* **2022**, *9*, 251. [CrossRef]
28. Baugh, C.; Colonese, J.; D'Angelo, C.; Dottori, F.; Neal, J.; Prudhomme, C.; Salamon, P. Global River Flood Hazard Maps. [Dataset]. 2024. Available online: http://Data.Europa.Eu/89h/Jrc-Floods-Floodmapgl_rp50y-Tif (accessed on 23 October 2024).
29. Van Der Knijff, J.M.; Younis, J.; De Roo, A.P.J. LISFLOOD: A GIS-based Distributed Model for River Basin Scale Water Balance and Flood Simulation. *Int. J. Geogr. Inf. Sci.* **2010**, *24*, 189–212. [CrossRef]
30. Falalakis, G.; Gemtzi, A. A Simple Method for Water Balance Estimation Based on the Empirical Method and Remotely Sensed Evapotranspiration Estimates. *J. Hydroinform.* **2020**, *22*, 440–451. [CrossRef]
31. Pisinaras, V.; Polychronis, C.; Gemtzi, A. Intrinsic Groundwater Vulnerability Determination at the Aquifer Scale: A Methodology Coupling Travel Time Estimation and Rating Methods. *Environ. Earth Sci.* **2016**, *75*, 85. [CrossRef]
32. Kofidou, M.; Gemtzi, A. Assimilating Soil Moisture Information to Improve the Performance of SWAT Hydrological Model. *Hydrology* **2023**, *10*, 176. [CrossRef]
33. FAO. *UNESCO Soil Map of the World—Australasia*; FAO: Paris, France, 1978.
34. Yassoglou, N.; Tsadilas, C.; Kosmas, C. *The Soils of Greece*; World Soils Book Series; Springer International Publishing: Cham, Switzerland, 2017; ISBN 978-3-319-53332-2.
35. Koimtzidis, M.; Makridis, A.; Fang, B.; Lakshmi, V.; Gemtzi, A. Modeling Net Primary Productivity Using near Real Time Land Cover Data and Soil Moisture Information. *Remote Sens. Lett.* **2024**, *in press*, accepted manuscript. [CrossRef]
36. *Special Secretariat for Water Flood Hazard Management Plan (Basins of the Water District of Thrace)*; Ministry of Environment and Energy: Athens, Greece, 2018.
37. Dimitriou, E.; Efstratiadis, A.; Zotou, I.; Papadopoulos, A.; Iliopoulou, T.; Sakki, G.-K.; Mazi, K.; Rozos, E.; Koukouvinos, A.; Koussis, A.D.; et al. Post-Analysis of Daniel Extreme Flood Event in Thessaly, Central Greece: Practical Lessons and the Value of State-of-the-Art Water-Monitoring Networks. *Water* **2024**, *16*, 980. [CrossRef]
38. Google and World Resources Institute Dynamic World App. Available online: <https://dynamicworld.app/> (accessed on 25 March 2024).
39. Mentzafou, A.; Markogianni, V.; Dimitriou, E. The Use of Geospatial Technologies in Flood Hazard Mapping and Assessment: Case Study from River Evros. *Pure Appl. Geophys.* **2017**, *174*, 679–700. [CrossRef]
40. European Commission Directorate-General for Agriculture and Rural Development. *Typology Handbook*; European Commission Directorate: Athens, Greece, 2020.
41. European Investment Bank Greece. *EIB Backs EUR 355m Scheme to Protect Cities from Floods and Climate Change*; European Investment Bank Greece: Athens, Greece, 2019.
42. Poulos, S.; Karditsa, A.; Hatzaki, M.; Tsapanou, A.; Papapostolou, C.; Chouvardas, K. An Insight into the Factors Controlling Delta Flood Events: The Case of the Evros River Deltaic Plain (NE Aegean Sea). *Water* **2022**, *14*, 497. [CrossRef]
43. Büttner, G. CORINE Land Cover and Land Cover Change Products. In *Land Use and Land Cover Mapping in Europe: Practices & Trends*; Manakos, I., Braun, M., Eds.; Springer: Dordrecht, The Netherlands, 2014; pp. 55–74. ISBN 978-94-007-7969-3.
44. Iyer, P.; Bozzola, M.; Hirsch, S.; Meraner, M.; Finger, R. Measuring Farmer Risk Preferences in Europe: A Systematic Review. *J. Agric. Econ.* **2020**, *71*, 3–26. [CrossRef]
45. Mavroulis, S.; Mavrouli, M.; Lekkas, E.; Tsakris, A. Impact of the September 2023 Storm Daniel and Subsequent Flooding in Thessaly (Greece) on the Natural and Built Environment and on Infectious Disease Emergence. *Environments* **2024**, *11*, 163. [CrossRef]
46. Greek Ministry of Agriculture. *Hellenic Organization of Agricultural Compensations*; Greek Ministry of Agriculture: Athens, Greece, 2023.
47. Naftemporiki. Unprecedented Flood Disaster in Thessaly. Available online: <https://www.naftemporiki.gr/finance/economy/1513193/asyllipti-i-katastrofi-se-georgia-kai-ktinotrofia-apo-tis-plimmyres/> (accessed on 23 October 2024). (In Greek).
48. Business Daily Increasing Costs of Large Infrastructure Works in Thessaly. Available online: https://www.businessdaily.gr/oikonomia/109504_ektosexetai-os-ta-45-dis-eyro-kostos-ton-megalon-ergon-sti-thessalia (accessed on 23 October 2024). (In Greek).

Disclaimer/Publisher's Note: The statements, opinions and data contained in all publications are solely those of the individual author(s) and contributor(s) and not of MDPI and/or the editor(s). MDPI and/or the editor(s) disclaim responsibility for any injury to people or property resulting from any ideas, methods, instructions or products referred to in the content.